https://doi.org/10.5194/angeo-2020-5
Preprint. Discussion started: 2 March 2020

Annales Geophysicae Discussions

Ionospheric total electron content anomaly possibly associated with the April 4, 2010 Mw7.2 Mexico earthquake

Jing Liu[1, 2], Wenbin Wang[2], and Xuemin Zhang[1]

[1]*Institute of Earthquake Forecasting, China Earthquake Administration, Beijing, China*

[2]*High Altitude Observatory, National Center for Atmospheric Research, Boulder, Colorado, USA*

Corresponding author: Jing Liu, Institute of Earthquake Forecasting, China Earthquake Administration, No. 63 Fuxing Road, Haidian district, Beijing 100036, China. (liujingeva@163.com)

Abstract

Identifying ionospheric disturbances potentially related to an earthquake is a challenging work. Based on the ionospheric total electron content (TEC) data from the madrigal database at the Haystack Observatory, Massachusetts Institute of Technology, a new decomposition and nonlinear fitting method has been developed and applied in this work to extract the TEC disturbances that are potentially related to the Mw7.2 Mexico earthquake occurred on April 4 2010. By analyzing the TEC data for a long period of time (72 days) before and after the earthquake, we found that a unique TEC depletion occurred in the region around the epicenter on March 25. No other significant ionospheric TEC anomalies were identified in the 72-day period around the earthquake, except some TEC disturbances that appeared to be related to the geomagnetic activity between April 1 and 6, 2010. We further analyzed the TEC data from other magnetically quiet days, and no TEC anomaly like that occurred on

https://doi.org/10.5194/angeo-2020-5
Preprint. Discussion started: 2 March 2020

March 25 was detected. The TEC data calculated from a first principles model SD-WACCM-X were also analyzed using the same method as that for the observational data. No TEC anomaly was found on March 25 from the model outputs either. Thus the source of the TEC anomaly on March 25 is unlikely from the lower atmosphere waves. In this study, we show the occurrence of TEC anomaly on March 25, 10 days before the Mw7.2 Mexico earthquake and this TEC anomaly may not be explained by lower atmosphere or geomagnetic activity forcing.

Key words: GPS TEC, ionospheric TEC anomaly, Mw7.2 Mexico earthquake

1. Introduction

The abnormal ionospheric density variations before and/or after earthquakes have attracted much attention from the geophysicists for many years (e.g., Pulinets & Boyarchuk, 2004a; Le et al., 2015). However, identifying and determining ionospheric density disturbances that are associated with an earthquake have been challenging so far. For instance, Heki (2011) reported the enhancement of ionospheric total electron content (TEC) ~40 min before the 2011 Mw9.0 Tohoku-oki earthquake. However, in subsequent studies, some scientists questioned the true cause of this pre-seismic abnormity in their comments (Kamogawa and Kakinami, 2013; Utada and Shimizu, 2014; Masci et al., 2015). Heki and Enomoto (2013, 2015) later applied several data analysis methods and more case studies to demonstrate the correlation between pre-seismic TEC abnormity and the earthquake. Despite these controversies, several data analysis methods have been employed to explore potential

https://doi.org/10.5194/angeo-2020-5
Preprint. Discussion started: 2 March 2020

seismo-ionospheric perturbations in previous studies. The running mean method is a common approach in analyzing time series data. Liu et al. (2000) utilized the running median of the critical frequency of the ionospheric F_2 layer (foF_2) and the inter-quartile range (IQR) of foF_2 as the upper and lower bounds to extract seismo-ionospheric precursors that may be associated with M≥6.0 earthquakes around Taiwan from 1994 to 1999. Pulinets et al. (2005) calculated the monthly mean (M) of ionospheric TEC, and used $M \pm \sigma$ as the thresholds to find TEC disturbances before the Colima Mexico earthquake, where σ is the standard deviation. In order to obtain the location characteristics of the ionospheric perturbations associated with earthquakes, spatial analysis methods have been applied in some researches. Liu et al. (2011) studied the locations of extreme TEC anomalies (enhancements or depletions) in the 12 2-hour intervals for a day. They compared the data with previous 30-day data in each grid to determine if they are maximum or minimum values in that 30-day period, and to see whether these TEC anomalies occur only nearby the earthquake region or randomly worldwide. Liu et al. (2016) found, by calculating the spatial relative changes, that ionospheric TEC, electron and ion densities were simultaneously enhanced at different altitudes near the epicenter of the 2005 Sumatra Indonesia Ms 7.2 earthquake. A correlation analysis between different stations was applied to demonstrate the local disturbance near the epicenter. Pulinets et al. (2004b) calculated the cross-correlation coefficient between two measurement points located inside or outside the earthquake preparation zone, and found that the coefficient sharply dropped before strong seismic shocks. Iwata and Umeno (2016) detected the preseismic TEC anomalies before the main shock, foreshock and aftershock of 2011 Tohoku-Oki *Mw* 9.0 earthquake by correlation analysis.

Statistics analysis of seismo-ionospheric disturbances has also been attempted by scientists when there are sufficient data. Liu et al. (2010) utilized the *z*-test for 150 M≥5.0 earthquakes during 2001-2007 to try to correlate the change of the ionospheric equatorial ionization anomaly (EIA) with earthquakes. Parrot (2012) applied a software to automatically detect the abrupt enhancement of ion density observed by the Detection of Electro-Magnetic Emissions Transmitted from Earthquake Regions (DEMETER) satellite. Based on the statistical analysis of 17,366 M>4.8 earthquakes, he found that perturbations in ionospheric ion density before earthquakes are more obvious than those prior to random selected pseudo-earthquake events. Therefore, there is not a unified and standard method to extract ionospheric density anomalies that may be related to earthquakes.

The ionosphere shows strong variability of different temporal and spatial scales. This variability can be of different sources, including the effects of large-scale lower atmospheric waves, geomagnetic and solar activity, and possibly, the earthquakes. Some ionospheric oscillations have known periods and zonal structures (e.g., Forbes et al., 2008; Pancheva & Mukhtarov, 2012; Luan et al., 2012). In this study, we use a new approach to extract possible ionospheric anomalies related to earthquakes. We obtain TEC residuals by removing the known and identified oscillations in the ionosphere TEC data. Since earthquakes are mostly single occurrence events at particular locations and times, these TEC residuals

https://doi.org/10.5194/angeo-2020-5
Preprint. Discussion started: 2 March 2020

can manifest earthquake effects on the ionosphere better. We use the TEC data from the madrigal database at the Massachusetts Institute of Technology (MIT) Haystack Observatory. The TEC data have high temporal resolution from a significantly large number of Global Position System (GPS) stations (about 1500 sites from 2000, now almost 6000 sites) all over the world. Therefore, the database can provide high temporal and spatial resolution data for our analysis. In this paper, section 2 describes the data and analysis method. In section 3, MIT TEC data before and after the Mw7.2 Mexico earthquake occurred on April 4 2010 are analyzed to obtain ionospheric TEC perturbations. In section 4, we use more observational data from other time periods and first principles numerical simulations by SD-WACCM-X to show the uniqueness of the TEC disturbances that occurred before the Mw7.2 Mexico earthquake. Finally, the conclusions are drawn in section 5.

2. Observations and the Method for Data Analysis

Based on a network of worldwide GPS receivers, MIT TEC is calculated by using an automated software suite (Rideout & Coster, 2006). It includes downloading data, determining satellite and receiver biases, removing data outliers, mapping from slant TEC to vertical TEC, and so on. The data are provided as estimates of vertical TEC in 1° by 1° grids distributed around locations where data are available. The temporal resolution of the TEC maps is 5 minutes. The advantage of MIT TEC is that it is strictly data driven with no underlying models that smooth out the real gradients in the TEC. In this

https://doi.org/10.5194/angeo-2020-5
Preprint. Discussion started: 2 March 2020

study, the TEC data are downloaded from the MIT Haystack Observatory madrigal database (http://madrigal.haystack.mit.edu/madrigal/).

The Fast Fourier Transform (FFT) algorithm was applied to obtain the spectral distribution of the TEC mean value in the northern American region (20°N-50°N in latitude, 90°W-140°W in longitude) from 2000 to 2017 (Figure 1). Multi-day spectral peaks are seen in the figure, including 27-day solar rotation, semiannual and annual oscillations. The high-frequency tidal spectral peaks at 24-hour (diurnal), 12-hour (semidiurnal), 8-hour (terdiurnal) and 6-hour (quad diurnal) are also obvious in Figure 1. The TEC data in each day can be expressed as a superposition of tide-like components (Forbes et al., 2008; Luan et al., 2012). In this paper we used Eq. (1) to express TEC data, which includes 6 terms:

$$f(t)=A(0)+A(1)*\cos\left(\frac{2\pi}{24}t+B(1)\right)+A(2)*\cos\left(\frac{2\pi}{12}t+B(2)\right)+A(3)*\cos\left(\frac{2\pi}{8}t+B(3)\right)$$
$$+A(4)*\cos\left(\frac{2\pi}{6}t+B(4)\right)+A(5) \qquad (1)$$

where A(0) is the daily mean TEC, A(1), A(2), A(3), A(4) and B(1), B(2), B(3), B(4) are the amplitudes and phases of diurnal, semidiurnal, terdiurnal, and 6-hour oscillations, respectively. A(5) is the residual, which includes higher frequency oscillations and/or some unknown variability, for example, the perturbations caused by an earthquake. In this study, three steps were taken to obtain A(5). First, if there were extremely large values in the raw data, which may be caused by data error, the data were canceled at its observation time. Second, a linear fitting between the solar 10.7 cm radio flux index ($F_{10.7}$), the

https://doi.org/10.5194/angeo-2020-5
Preprint. Discussion started: 2 March 2020

Annales Geophysicae Discussions Open Access

geomagnetic activity index (*AE*) and the TEC data was applied to remove solar and magnetic activity effects. Similar to Pi et al. (2003) and Lei et al (2004), who used nonlinear least square minimization to minimize the difference between the model results and observational data to investigate the mechanisms of ionospheric variations, we also employed a nonlinear fitting method to obtain the coefficients in Eq. (1) for each day in the third step. The data would not be fitted if the number of data in a day is less than 72 (the total number of data is 288 for each day at the 5-minute cadence) and if the data gaps are larger than 6 hours. A running mean method was applied to do these fitting, with 1-day window and 1-hour step, which means there will be 24 fitted data in each day. From these three steps, A(5) was extracted using Eq. (1) to analyze the TEC changes before and after the earthquake. Hereafter, we will show TEC residual values of A(5) obtained from the above described data analysis processes.

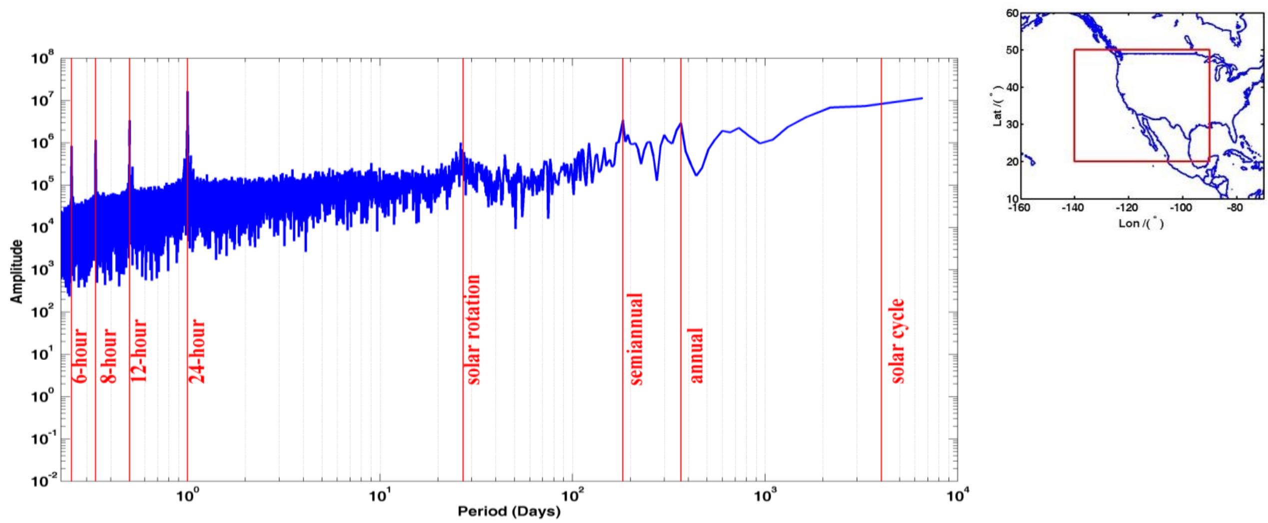

Figure 1: The FFT spectrum of the TEC mean values from 2000 to 2017 in the North American region (20°N-50°N in latitude, 90°W-140°W in longitude), which is shown with the red rectangle in the subplot.

https://doi.org/10.5194/angeo-2020-5
Preprint. Discussion started: 2 March 2020

3. Results

The Mexico Mw7.2 earthquake with 10 km depth occurred at 22:40 UT (universal time) on April 4 2010. The epicenter was located at (32.286°N, 115.295°W). The TEC data around the epicenter in a region with latitude from 30°N-34°N and longitude from 113°W-117°W were obtained and analyzed from March 14 to April 6, 2010. The mean TEC residual in this region is shown in the bottom panel of Figure 2. From the time series of $F_{10.7}$ and geomagnetic activity indices (*K*p, *D*st, and the *AE*) in Figure 2, it can be seen that there was no geomagnetic activity from March 14 to March 31. It became more active since April 1, especially after April 5 when *D*st dropped to below -40 nT.

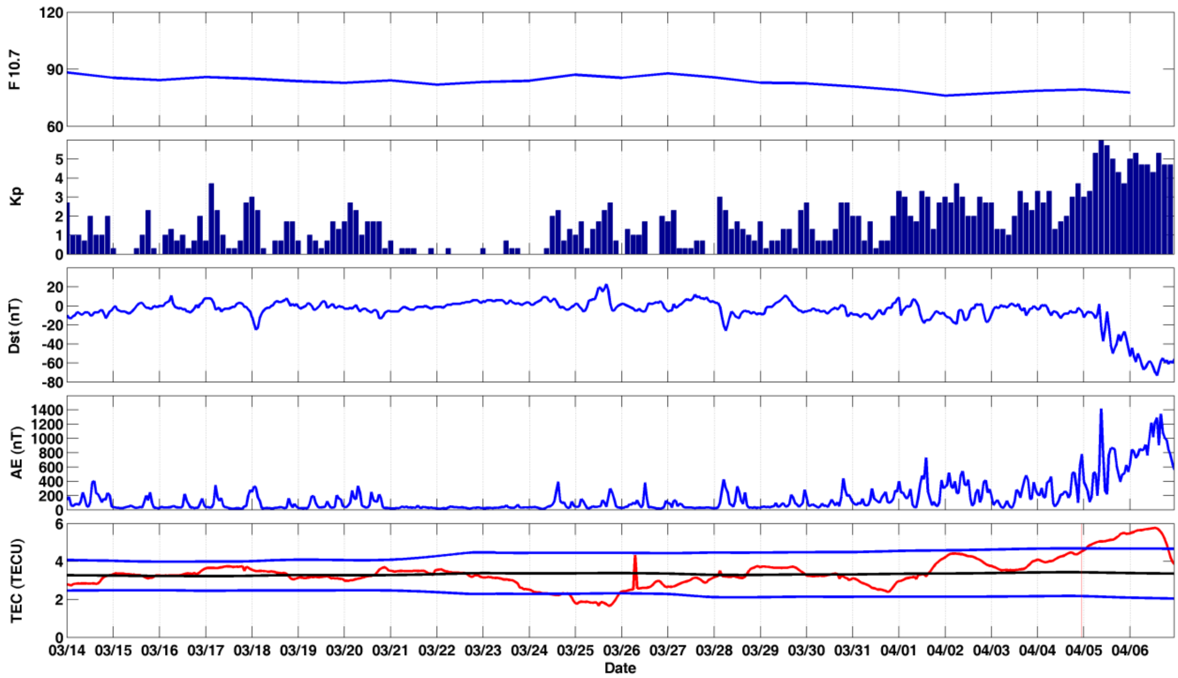

Figure 2: Time series of TEC residual (A(5)) around the epicenter from March 14 to April 6, 2010. Panels from top to bottom represent time series of $F_{10.7}$, *K*p, *D*st, the *AE* index and TEC residual, respectively. In the bottom panel, the red

https://doi.org/10.5194/angeo-2020-5
Preprint. Discussion started: 2 March 2020

line is the mean value of the TEC residual in the region of latitude 30°N-34°N and longitude 113°W-117°W. The black and blue lines represent the mean values and M±1.5*σ of ±15 days of data centered around a particular day. The vertical red line on April 4 indicates the occurrence time of the Mexico Mw7.2 earthquake.

Under the assumption of a normal distribution, the probability of data in the range of ±σ and ±2σ is 68.26% and 95.44%, respectively. In order to avoid the probability being too low or high, we used M±1.5*σ (the probability is 86.64%) as the threshold to extract the disturbances that may be related to earthquakes, where M and σ stands for the mean value and standard deviation of TEC residuals of ±15 days centered around a particular day, respectively. Before the Mexico earthquake, the TEC value was lower than the threshold on March 25. In other days from March 14 to April 5, TEC residual value for each day was within the thresholds. When magnetic activity became stronger, the TEC was also increasing with the values over the upper bound from April 5 to 6. Therefore, except the depletion of TEC residual on March 25 and the increase of TEC residual associated with the magnetic activity on April 5 and 6, no TEC anomalies exceeding the thresholds were detected in other days during the 72-day period.

In order to further analyze the TEC changes potentially related to the earthquake, we expanded the region of interest to include the area of latitude 20°N-50°N and longitude 90°W-140°W. In this analysis of TEC spatial structure, the differences between the TEC residuals and the mean values of ±15-day data for a particular day were obtained before and after the earthquake. For each day, the mean value of

https://doi.org/10.5194/angeo-2020-5
Preprint. Discussion started: 2 March 2020

Annales Geophysicae Discussions

the 24-hour data was used to represent the TEC residual, as shown in Figure 3. The TEC depletion on March 25 is evident in the region surrounding the epicenter, similar to the analysis result of the time series shown in Figure 2. The TEC depletion can also be seen south and west to the epicenter. In all the days shown in Figure 3, only on March 25 did the TEC residual data show depletion in the region around the epicenter. The TEC residuals began to increase from April 1 in the western and southern part of the region. Large TEC values occurred in a large region when magnetic activity became strong on April 5 and 6.

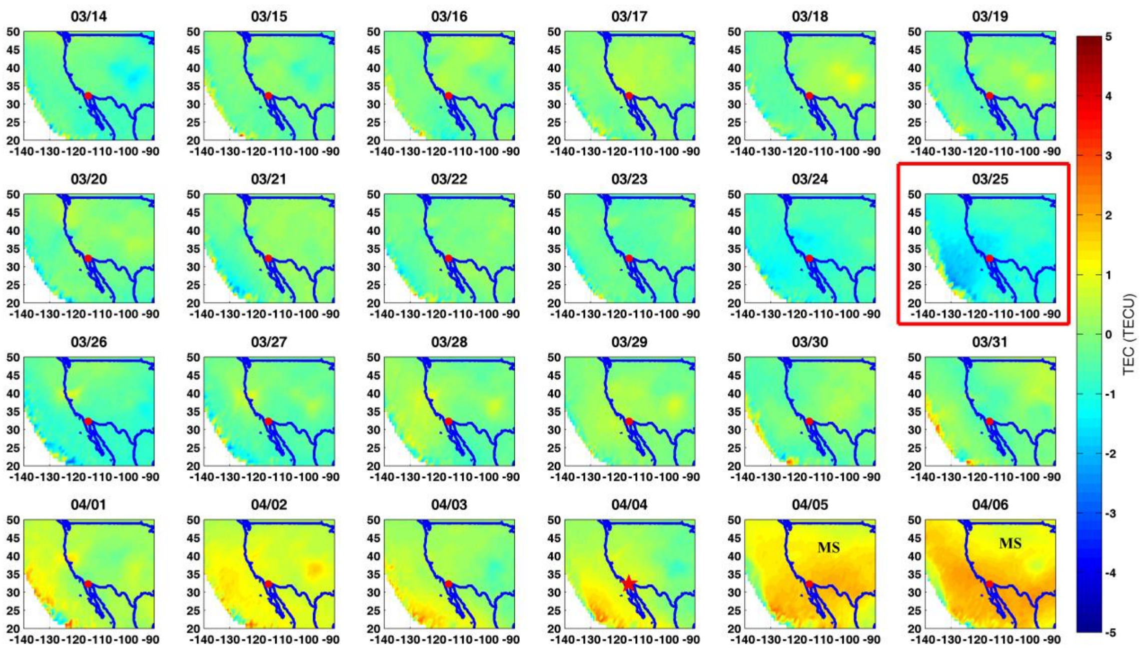

Figure 3: TEC changes in the region of latitude 20°N-50°N and longitude 90°W-140°W from March 14 to April 6, 2010. The red dot indicates the epicenter. The red star shows the day of the earthquake. The blue lines represent the continent. ‘MS’ on April 5 and 6 mean ‘magnetic storm’. The date of the map is marked on the top of each subpanel. The subpanel on March 25 is highlighted with the red rectangle.

https://doi.org/10.5194/angeo-2020-5
Preprint. Discussion started: 2 March 2020

4. Discussion

In order to further establish the possible correlation between the TEC depletion on March 25 and the Mexico Mw7.2 earthquake on April 4, we carried out a number of detailed analysis of the TEC variations in the region. Firstly, the analysis time was extended to more days before March 14 and after April 6 to determine the TEC changes over a longer period of time. The results are given in Figures 4 and 5. We can see that, except the TEC decrease on April 11 when a magnetic storm occurred with a minimum *D*st value of -55 nT, there were no extremely high or low TEC values in the region for all the days. Therefore, we can see from Figures 3-5 that, in 72 days from February 18 to April 30, there were four days of TEC anomalies: TEC depletion on March 25 under geomagnetically quiet conditions, TEC enhancements on April 5 and 6 under geomagnetically active conditions, and TEC depletion on April 11 under geomagnetic storm conditions. The unique occurrence of TEC depletion on the geomagnetically quiet day of March 25 is thus potentially connected to the occurrence of the earthquake on April 4 in the same region.

https://doi.org/10.5194/angeo-2020-5
Preprint. Discussion started: 2 March 2020

Annales Geophysicae
Discussions
Open Access

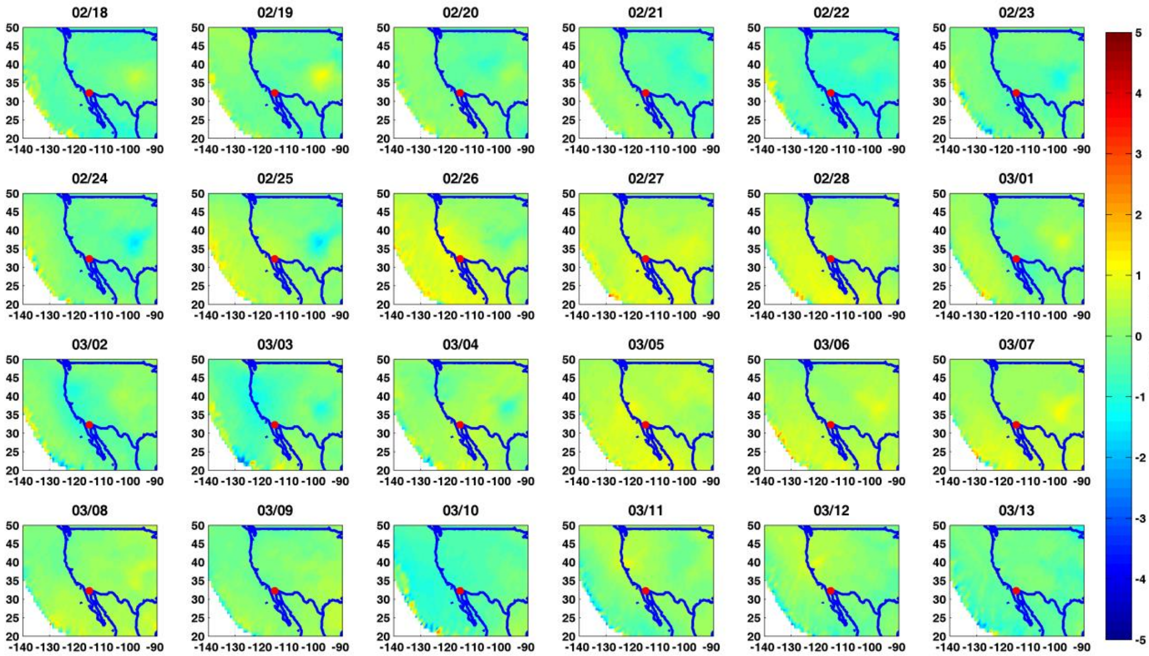

Figure 4: Same as Figure 3, but for February 18 to March 13, 2010.

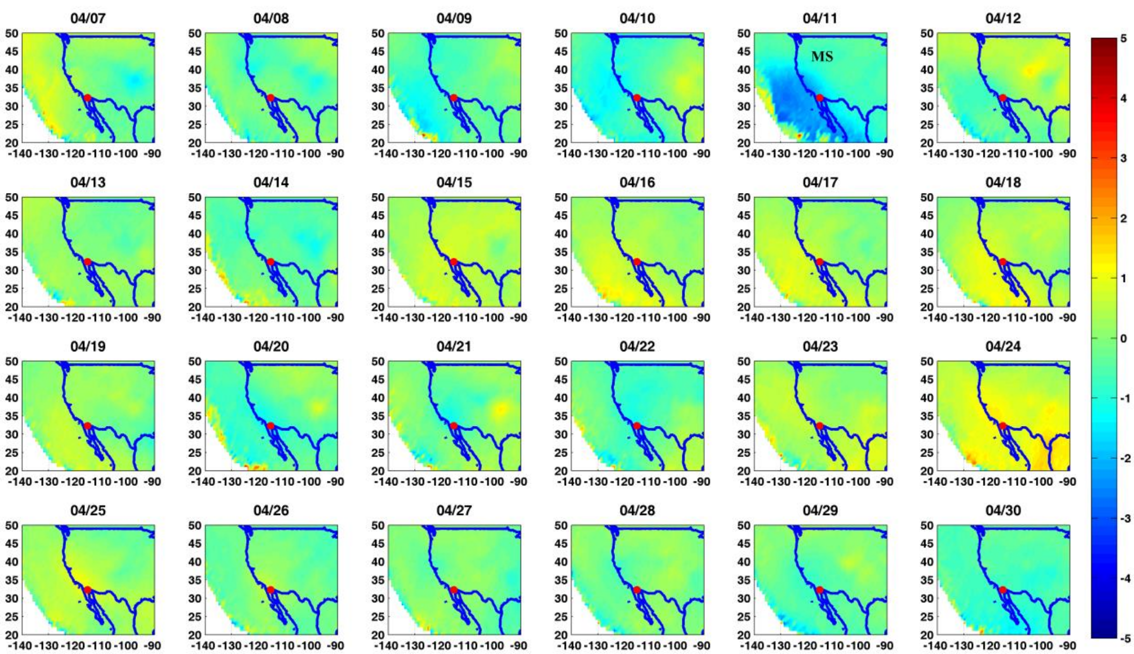

Figure 5: Same as Figure 3, but for April 7 to April 30, 2010.

https://doi.org/10.5194/angeo-2020-5
Preprint. Discussion started: 2 March 2020

Secondly, we analyzed the TEC changes in the geomagnetically quiet days of other years (-30 nT < *D*st < 20 nT, *K*p < 3, *AE*<500 nT) using the same analysis method described above. We found that the time period from November 27 2009 to January 19 2010 was geomagnetically quiet and there were continuous TEC data to allow a meaningful data analysis. In this study, since we use ±15 days data as the background, the first day with analysis results should be 15 days later than November 27 2009. The distribution of the differences of TEC residuals from December 12 2009 to January 4 2010 is given in Figure 6. There was no TEC anomaly in all those days, which means that when geomagnetic activity is quiet, the TEC anomaly seen on March 25 before the Mexico Mw7.2 earthquake may not appear.

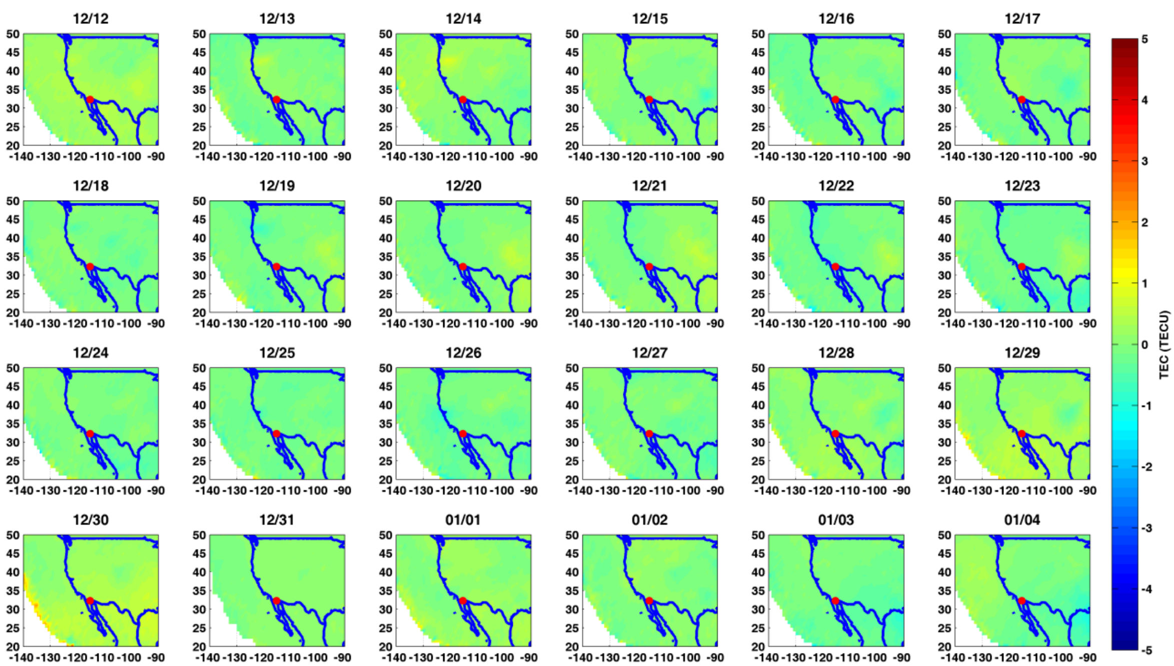

Figure 6: Same as Figure 3, but for December 12 2009 to January 4 2010 in geomagnetically quite days.

Thirdly, it is important to distinguish the seismic disturbance and the medium-scale traveling ionospheric disturbances (MSTIDs). Iwata and Umeno (2017) calculated the rate of anomalous area and the propagation velocity to detect the preseismic ionospheric disturbances. Otsuka et al. (2011) reported that the propagation of atmospheric gravity waves and auroral activity are the main sources of the MSTIDs. In this study, first principles simulations were employed to further examine the potential source of the TEC anomaly seen on March 25, 2010, especially the lower atmospheric waves. Here we used the thermosphere and ionosphere extension of the Whole Atmosphere Community Climate Model (WACCM-X) (Liu et al., 2018). The top boundary of WACCM-X is set at 4.0×10^{-10} hPa (~500 to ~700 km altitude, depending on solar activity). WACCM-X can well simulate the chemical and physical processes in the atmosphere (Marsh et al., 2013; Neale et al., 2013). WACCM-X can be configured either for free climate simulations (lower atmosphere unconstrained), or to have the tropospheric and stratospheric dynamics constrained to meteorological reanalysis fields for specifically targeted time periods. The later one is called specified dynamics WACCM-X (SD-WACCM-X, Sassi et al., 2013). A detailed description of the SD-WACCM-X can be found in Marsh (2011). With the lower atmospheric dynamics constrained by the observational data, SD-WACCM-X can accurately represent the large-scale and medium-scale lower atmospheric waves that can propagate upward and affect the thermosphere and ionosphere. In this study, we used the SD-WACCM-X to determine whether the TEC depletion seen on March 25 is related to lower atmospheric forcing. The SD-WACCM-X has a

https://doi.org/10.5194/angeo-2020-5
Preprint. Discussion started: 2 March 2020

Annales Geophysicae
Discussions
Open Access

horizontal resolution of 1.9° in latitude and 2.5° in longitude. Using the same data analysis method described in section 2, the distributions of the differences of the simulated TEC residual from March 14 to April 6, 2010 are shown in Figure 7 within the region of latitude 20°N-50°N and longitude 90°W-140°W to be consistent with the data. Except the TEC enhancements around the northern crest of EIA on April 5, no TEC anomaly is identified around the epicenter. The TEC depletion on March 25 is not detected in SD-WACCM-X outputs, which means that the TEC anomaly source may not result from the lower atmospheric forcing.

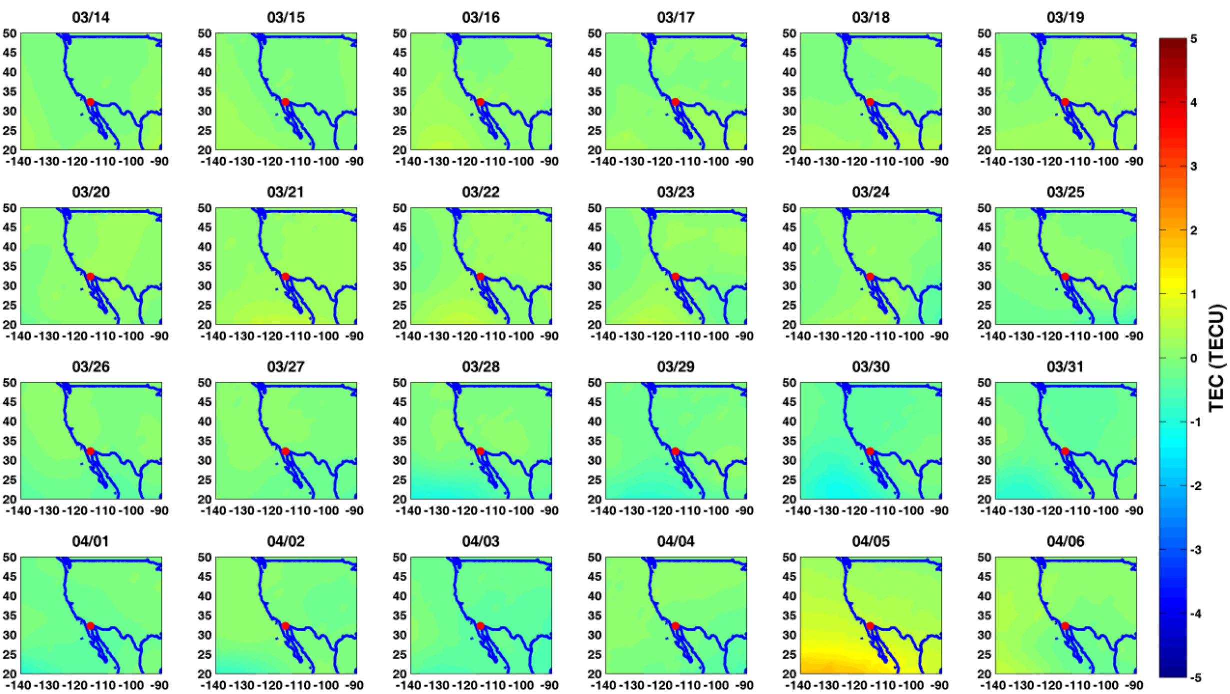

Figure 7: Same as Figure 3, but for SD-WACCM-X outputs from March 14 to April 6, 2010.

Takeuchi et al. (2006) pointed out that the stress of the p-holes in the crust can reach the surface and create an upward electric field. Pulinets and Ouzounov (2011) supported the hypothesis of atmospheric electricity changes caused by radon emanation and air ionization near the fault zone. Sorokin et al. (2005) suggested that the DC electric field that forms above seismically active regions could penetrate into the ionosphere. Kuo et al. (2011, 2014) proposed the electrical coupling between the ionosphere and the surface charges in the earthquake fault zone. They suggested that the vertical surface electric field drives currents in the atmosphere and electric fields at the bottom of the ionosphere. If there is an upward electric field in the ionosphere, with the $\boldsymbol{E} \times \boldsymbol{B}$ drifts, the plasma moves westward. Furthermore, Pulinets and Boyarchuk (2004a) suggested that the seismo-ionospheric phenomena did not coincide with the vertical projection of the epicenter, but shifted equatorward. In our study, we found that the depletion of TEC residuals occurred not only over the epicenter but also south and west to the epicenter, which may be related to the above mentioned lithosphere-atmosphere-ionosphere coupling.

5 Conclusions

In this study, we applied a decomposition and nonlinear fitting method on the MIT TEC data to obtain ionospheric TEC anomaly that is possibly associated with earthquakes. We analyzed the MIT TEC data near the Mexico Mw7.2 earthquake that occurred on April 4 2010. We also carried out numerical simulations using first principles model SD-WACCM-X. The main conclusions of this work are as follows:

The TEC decreased on March 25 around the epicenter, 10 days before the earthquake. Except for the TEC perturbations that were clearly related to geomagnetic activity, no TEC anomaly similar to that on March 25 was seen in other 68 days around the day of the earthquake. Furthermore, the TEC anomaly seen on March 25 cannot be found in geomagnetically quite days from December 12 2009 to January 4 2010 in the same region, either.

The TEC simulated by the SD-WACCM-X runs did not show TEC decrease around the epicenter on March 25. SD-WACCM-X includes lower atmospheric large-scale waves and their coupling effects on the ionosphere. Therefore, the model results suggest that the ionosphere TEC anomaly on March 25 might not be the result of lower atmospheric forcing. Our data analysis and model simulations thus indicate that the TEC anomaly seen on March 25 may be potentially related to the Mexico Mw7.2 earthquake.

Although we identify ionospheric anomalies (TEC depletion) that are possibly associated with the 2010 Mexico Mw7.2 earthquake in this work, more case studies and physics-based simulations are needed in the future to fully understand the physical mechanism of the seismo-ionospheric coupling.

Acknowledgments

This work is supported by the National Key R&D Program of China (2018YFC1503506), the APSCO Earthquake Research Project Phase Ⅱ, the China Scholarship Fund and ISSI-Beijing. The authors acknowledge the madrigal database at the Massachusetts Institute of Technology Haystack

Observatory for providing the GPS TEC data, and the data can be downloaded from http://madrigal.haystack.mit.edu/madrigal/. The authors acknowledge the WACCM-X development teams at NCAR. The WACCM-X is an open-source community model. The outputs from model runs used in this study are calculated using the NCAR supercomputer. NCAR is sponsored by the National Science Foundation.

Data availability

The MIT TEC data can be downloaded from http://madrigal.haystack.mit.edu/madrigal/.

Author contribution

Jing Liu analyzed the data and writed the manuscript. Wenbin Wang proposed the topic, conceived and designed the study. Xuemin Zhang helped in the interpretation. All authors read and approved the final manuscript.

Competing interests

The authors declare that they have no competing interest.

Statement

The journal of Annales Geophysicae has the right to reproduce materials in this manuscript, including figures, tables, and maps.

Reference

Forbes, J. M., Zhang, X., Palo, S., Russell, J., Mertens, C. J., and Mlynczak, M.: Tidal variability in the ionospheric

https://doi.org/10.5194/angeo-2020-5
Preprint. Discussion started: 2 March 2020

Annales Geophysicae Discussions
Open Access
EGU

dynamo region, J. Geophys. Res., 113, A02310, doi:10.1029/2007JA012737, 2008.

Heki, K.: Ionospheric Electron Enhancement Preceding the 2011 Tohoku-Oki Earthquake, Geophysical Research Letters, 38, L17312, doi:10.1029/2011GL047908 (2011),.

Heki, K., and Enomoto, Y.: Preseismic ionospheric electron enhancements revisited, J. Geophys. Res. Space Physics, 118, 6618-6626, doi:10.1002/jgra.50578, 2013.

Heki, K., and Enomoto, Y.: Mw dependence of the preseismic ionospheric electron enhancements, J. Geophys. Res. Space Physics, 120, 7006-7020, doi:10.1002/2015JA021353, 2015.

Iwata, T., Umeno, K.: Correlation analysis for preseismic total electron content anomalies around the 2011 Tohoku-Oki earthquake, J. Geophys. Res. Space Physics, 121(9), 8969-8984, 2016.

Iwata, T., Umeno, K.: Preseismic ionospheric anomalies detected before the 2016 Kumamoto earthquake, J. Geophys. Res. Space Physics, 122(3), 3602-3616, 2017.

Kamogawa, M., and Kakinami, Y.: Is an ionospheric electron enhancement preceding the 2011 Tohoku-oki earthquake a precursor? J. Geophys. Res. Space Physics, 118, 1-4, doi:10.1002/jgra.50118, 2013.

Kuo, C., Huba, J., Joyce, G., and Lee, L.: Ionosphere plasma bubbles and density variations induced by pre-earthquake rock currents and associated surface charges, J. Geophys. Res., 116, A10317, doi:10.1029/2011JA016628, 2011.

Kuo, C. L., Lee, L. C., and Huba, J. D.: An improved coupling model for the lithosphere-atmosphere-ionosphere system, J. Geophys. Res. Space Physics, 119, 3189-3205, doi:10.1002/2013JA019392, 2014.

Le, H., Liu, J., Zhao, B. Q., and Liu, L. B.: Recent progress in ionospheric earthquake precursor study in China: A brief review, Journal of Asian Earth Sciences, 114, 420-430, 2015.

Lei, J., Liu, L., Wan, W., and Zhang, S.: Modeling the behavior of ionosphere above Millstone Hill during the September 21-27, 1998 storm, J Atmos Solar-Terr Phys, 66: 1093-1102, 2004.

Liu, H. L., Bardeen, C. G., Foster, B. T., Lauritzen, P., Liu, J., Lu, G…., and Wang, W.: Development and validation of the Whole Atmosphere Community Climate Model with thermosphere and ionosphere extension (WACCM-X

https://doi.org/10.5194/angeo-2020-5
Preprint. Discussion started: 2 March 2020

2.0), Journal of Advances in Modeling Earth Systems, doi:10. https://doi.org/10.1002/2017MS001232, 2018.

Liu, J., Chen, Y., Pulinets, S., Tsai, Y., and Chuo, Y.: Seismo-ionospheric signatures prior to M≥ 6.0 Taiwan earthquakes, Geophys. Res. Lett, 27(19), 3113-3116, 2000.

Liu, J., Chen, C., Chen, Y., Yang, W., Oyama, K., and Kuo, K.: A statistical study of ionospheric earthquake precursors monitored by using equatorial ionization anomaly of GPS TEC in Taiwan during 2001-2007, Journal of Asian Earth Sciences, 39(1), 76-80, 2010.

Liu, J., Le, H., Chen, Y., Chen, C., Liu, L., Wan, W., Su, Y., Sun, Y., Lin, C., and Chen, M.: Observations and simulations of seismoionospheric GPS total electron content anomalies before the 12 January 2010 M7 Haiti earthquake, J. Geophys. Res, 116, A04302, doi:10.1029/2010JA015704, 2011.

Liu, J., Zhang, X., Novikov, V., and Shen, X.: Variations of ionospheric plasma at different altitudes before the 2005 Sumatra Indonesia Ms 7.2 earthquake, J. Geophys. Res. Space Physics, 121(9), 9179-9187, doi:10.1002/2016JA022758, 2016.

Luan, X., Dou, X., Lei, J., and Jiang, G.: Terdiurnal migrating-tide signature in ionospheric total electron content. J. Geophys. Res., 117, A11302, doi:10.1029/2012JA018199, 2012.

Marsh, D. R.: Chemical-dynamical coupling in the mesosphere and lower thermosphere, in Aeronomy of the Earth's Atmosphere and Ionosphere, IAGA Spec. Sopron Book Ser., vol. 2, pp. 3-17, Springer, Heidelberg, Germany, doi:10.1007/978-94-007-0326-1_1, 2011.

Marsh, D. R., Mills, M. J., Kinnison, D. E., Lamarque, J.-F., Calvo, N., and Polvani, L. M.: Climate change from 1850 to 2005 simulated in CESM1 (WACCM), Journal of Climate, 26, 7372-7391. https://doi.org/10.1175/JCLI-D-12-00558.1, 2013.

Masci, F., Thomas, J. N., Villani, F., Secan, J. A., and Rivera, N.: On the onset of ionospheric precursors 40 min before strong earthquakes, J. Geophys. Res. Space Physics, 120, 1383-1393, doi:10.1002/2014JA020822, 2015.

Neale, R. B., Richter, J., Park, S., Lauritzen, P. H., Vavrus, S. J., Rasch, P. J., and Zhang, M.: The mean climate of the Community Atmosphere Model (CAM4) in forced SST and fully coupled experiments, Journal of Climate, 26, 5150-5168, https://doi.org/10.1175/JCLI-D-12-00236.1, 2013.

Otsuka, Y., Kotake, N., Shiokawa, K., Ogawa, T., Tsugawa, T., and Saito: A Statistical study of medium-scale traveling ionospheric disturbances observed with a GPS receiver network in Japan. In Aeronomy of the Earth's Atmosphere and Ionosphere, IAGA Spec. Sopron Book Ser., vol. 2, pp. 291-299, Springer, Netherlands, doi:10.1007/978-94-007-0326-1_21, 2011.

Pancheva, D., and Mukhtarov, P.: Global response of the ionosphere to atmospheric tides forced from below: Recent progress based on satellite measurements, Space Sci. Rev., 161, 175-209, doi:10.1007/s11214- 011-9837-1, 2012.

Parrot, M.: Statistical analysis of automatically detected ion density variations recorded by DEMETER and their relation to seismic activity, Annals of Geophysics, 55(1), 149-155, doi: 10.4401/5270, 2012.

Pi, X. , Wang, C. , Hajj, G. A. , Rosen, G. , Wilson, B. D. , and Bailey, G. J.: Estimation of E×B drift using a global assimilative ionospheric model: an observation system simulation experiment, Journal of Geophysical Research Space Physics, 108(A2), 1075-1088, 2003.

Pulinets, S., and Boyarchuk, K.: Ionospheric precursors of earthquakes, Springer Berlin Heidelberg, New York, 2004a.

Pulinets, S., Gaivoronska, T., Leyva Contreras, A., and Ciraolo, L.: Correlation analysis technique revealing ionospheric precursors of earthquakes, Natural Hazards and Earth System Sciences, 4, 697-702, 2004b.

Pulinets, S. A., Contreras, A. L., Bisiacchi-Giraldi, G., and Ciraolo, L.: Total electron content variations in the ionosphere before the Colima, Mexico, earthquake of 21 January 2003, Geofisica Internacional-Mexico, 44, 369-377, 2005.

Pulinets, S., and Ouzounov, D.: Lithosphere-Atmosphere-Ionosphere Coupling (LAIC) model - An unified concept for earthquake precursors validation, Journal of Asian Earth Sciences, 41, 371-382, doi:10.1016/j.jseaes.2010.03.005, 2011.

Sassi, F., Liu, H. L., Ma, J., and Garcia, R. R.: The lower thermosphere during the northern hemisphere winter of 2009:

https://doi.org/10.5194/angeo-2020-5
Preprint. Discussion started: 2 March 2020

A modeling study using high-altitude data assimilation products in WACCM-X, J. Geophys. Res. Atmos., 118, 8954-8968, doi:10.1002/jgrd.50632, 2013.

Sorokin, V., Yaschenko, A., Chmyrev, V., and Hayakawa, M.: DC electric field amplification in the mid-latitude ionosphere over seismically active faults, Nat. Hazards Earth Syst. Sci., 5, 661-666, doi:10.5194/nhess-5-661-2005, 2005.

Takeuchi, A., Lau, B. W. S., and Freund, F. T.: Current and surface potential induced by stress-activated positive holes in igneous rocks, Phys. Chem. Earth, Parts A/B/C, 31, 240-247, 2006.

Utada, H., and Shimizu, H.: Comment on “Preseismic ionospheric electron enhancements revisited” by K. Heki and Y. Enomoto, J. Geophys. Res. Space Physics, 119, 6011-6015, doi:10.1002/2014JA020044, 2014.